UCLA
UCLA Previously Published Works

Title

Ionic charge transport between blockages: Sodium cation conduction in freshly excised bulk brain tissue.

Permalink

https://escholarship.org/uc/item/6qw5f44j

Journal

AIP advances, 5(8)

ISSN

2158-3226

Authors

Emin, David
Akhtari, Massoud
Ellingson, BM
et al.

Publication Date

2015-08-01

DOI

10.1063/1.4928652

Peer reviewed

eScholarship.org Powered by the California Digital Library
University of California

Ionic charge transport between blockages: Sodium cation conduction in freshly excised bulk brain tissue

David Emin,[1,a] Massoud Akhtari,[2] B. M. Ellingson,[3] and G. W. Mathern[4]
[1]*Department of Physics and Astronomy, University of New Mexico, Albuquerque, NM 87131, USA*
[2]*Semple Institutes for Neuroscience and Human Behavior, David Geffen School of Medicine, University of California at Los Angeles, Los Angeles, CA 90095, USA*
[3]*Department of Radiology, David Geffen School of Medicine, University of California at Los Angeles, Los Angeles, CA 90095, USA*
[4]*Department of Neurosurgery, David Geffen School of Medicine, University of California at Los Angeles, Los Angeles, CA 90095, USA*

(Received 22 June 2015; accepted 3 August 2015; published online 11 August 2015)

We analyze the transient-dc and frequency-dependent electrical conductivities between blocking electrodes. We extend this analysis to measurements of ions' transport in freshly excised bulk samples of human brain tissue whose complex cellular structure produces blockages. The associated ionic charge-carrier density and diffusivity are consistent with local values for sodium cations determined non-invasively in brain tissue by MRI (NMR) and diffusion-MRI (spin-echo NMR). The characteristic separation between blockages, about 450 microns, is very much shorter than that found for sodium-doped gel proxies for brain tissue, > 1 cm. © *2015 Author(s). All article content, except where otherwise noted, is licensed under a Creative Commons Attribution 3.0 Unported License.* [http://dx.doi.org/10.1063/1.4928652]

Mapping and understanding ionic charge transport in defined regions of brain tissue is an essential element of neural research. Here we analyze the electrical conductivity of freshly excised bulk samples of brain tissue. Simple dc conductivity measurements exhibit a temporal decay. This temporal decay presumably results from the failure of ionic charge carriers to penetrate blockages. These dc conductivity measurements are complemented with conductivity measurements at low frequencies (6 – 1000 Hz). We analyze these measurements to estimate the dc limit of the electrical conductivity of brain tissues' ionic charge carriers and the characteristic separation between blockages to their flow. These estimates are consistent with sodium cation density and microscopic diffusivity determined non-invasively with MRI and diffusion-MRI.

Metallic electrodes generally function as extrinsic impenetrable barriers to ions' flow. In addition, intrinsic barriers can result from structural features of an inhomogeneous material that preclude the passage of ions on the time scale of a transport measurement.

First consider the temporal decay of the dc conductivity obtained with a circuit like that depicted schematically in Fig. 1. Current will flow within a homogeneous sample having blocking electrodes immediately following application of a spatially constant electric field at a time we define as zero. Initially carriers' flow will be characterized by their intrinsic dc conductivity σ_{dc}. However, the transient conductivity will decay from this initial value to zero as carriers are progressively stopped at the blocking electrode.

The non-uniform carrier density that results when the current flow ceases is determined by solving the corresponding charge-flow equation:

$$J(\infty) = 0 = \frac{nq^2D}{kT}E - qD\frac{dn}{dx}, \tag{1}$$

[a]Author to whom correspondence should be addressed. Electronic mail: emin@unm.edu

 ©Author(s) 2015

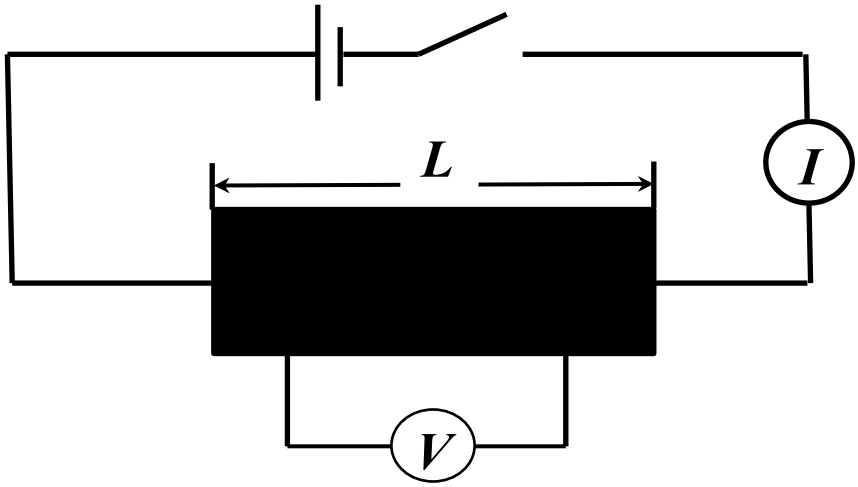

FIG. 1. Schematic illustration of our circuit for measuring the dc conductivity of a sample between blocking electrodes separated by the distance L.

where q, n and D respectively represent the carrier's charge, density and diffusion constant and E indicates the strength of the applied electric field. Here the carrier mobility μ is related to its diffusion constant by the Einstein relation, $\mu = qD/kT$, where k and T signify the Boltzmann constant and the temperature, respectively. Solving this first-order differential equation yields an expression for the resulting non-uniform spatial distribution of ions:

$$n(x,\infty) = n_e exp(qEx/kT), \tag{2}$$

where the maximum ion density occurs at the interface at which ions are blocked from exiting the material $x = L$ while the minimum ion density occurs at the opposing electrical contact at $x = 0$. The relationship between the constant n_e and the equilibrium carrier density n_0 is obtained by requiring constancy of the net number of ions:

$$n_0 L = n_e \int_0^L dx\, exp(qEx/kT) = n_e \frac{exp(qEL/kT) - 1}{(qE/kT)}. \tag{3}$$

Thus, at arbitrarily long times the non-uniform distribution of ions approaches

$$n(x,\infty) = n_0 \frac{(qEL/kT)}{exp(qEL/kT) - 1} exp(qEx/kT). \tag{4}$$

Structures from which charge can neither enter nor escape serve as "polarization centers." For example, an electronic charge carrier confined to an isolated pair of a semiconductor's dopants comprises a well-known polarization center.[1] Applying a constant electric field shifts centers' confined charges. The conductivity associated with this polarization decreases after the electric field is applied as $\exp(-t/\tau)$, where τ denotes the center's characteristic relaxation time.[1,2] This two-center relaxation time is calculated with the master equations in terms of the rates with which a carrier moves between sites.

A macroscopic sample whose mobile ions are confined by their inability to penetrate electrical contacts constitutes a macroscopic polarization center. In particular, with a sufficiently small carrier density one can ignore carriers' mutual interactions and generalize the two-center polarization current to account for multiple ionic carriers with multiple polarization distances. Then the macroscopic specimen's relaxation is described with the classical diffusion equation in terms of carriers' diffusion constant.[3]

The decaying conductivity is then modelled as the sum of contributions that each arises from a carrier's diffusing to its blockage. With the time characterizing a carrier's diffusing a distance l to

reach the blocking contact being $\tau(l) = l^2/2D$ this decaying conductivity becomes:

$$\sigma(t) = \frac{\sigma_{dc}}{L}\int_0^L dl e^{-t/\tau(l)} = \frac{\sigma_{dc}}{L}\int_0^L dl e^{-2Dt/l^2} = \sigma_{dc}\int_1^\infty du \frac{e^{-(2Dt/L^2)u}}{2u^{3/2}}$$
$$= \frac{\sigma_{dc}}{2} E_{3/2}(2Dt/L^2), \tag{5}$$

where $E_{3/2}(x)$ designates the established exponential integral defined in Eq. (5.1.4) of Ref. 4. As illustrated in Fig. 2, this transient conductivity monotonically falls from $\sigma_{\rm dc}$ at $t = 0$ toward zero with increasing time. In particular, this exponential integral's value at $t = 0$ is given by $E_{3/2}(0) = 1/[(3/2) - 1] = 2$. In the complementary long-time limit, $2Dt/L^2 \gg 1$, the dc conductivity's temporal decay is described by:

$$\sigma(t) \cong \sigma_{dc}\left[\frac{exp(-2Dt/L^2)}{(2Dt/L^2) + 3/2}\right]. \tag{6}$$

Distinctively, the relaxation time for interfacial conductivity produced by impenetrable electrodes decreases as the inter-electrode separation L is decreased. We observed the temporal decay of the ionic conductivities of samples of gelatin gels doped with NaCl. These NaCl-doped gels are commonly employed proxies for brain tissues in that their sodium cation concentrations and diffusion constants are close to those of human brain tissue. We witnessed the relaxation times ($10^2 - 10^3$ sec) falling as the sample length and the associated inter-electrode separation L is reduced. In these instances our metallic electrodes function as extrinsic impenetrable barriers that dominate the temporal decay of the conductivity.

Measurement of the real part of the frequency-dependent conductivity, via a circuit like that schematically depicted in Fig. 3, provides an alternative way of studying the transient decay of the conductivity. In particular, the real part of the frequency-dependent ac conductivity corresponding to this temporally decaying current is obtained from the Fourier transforms of the current density

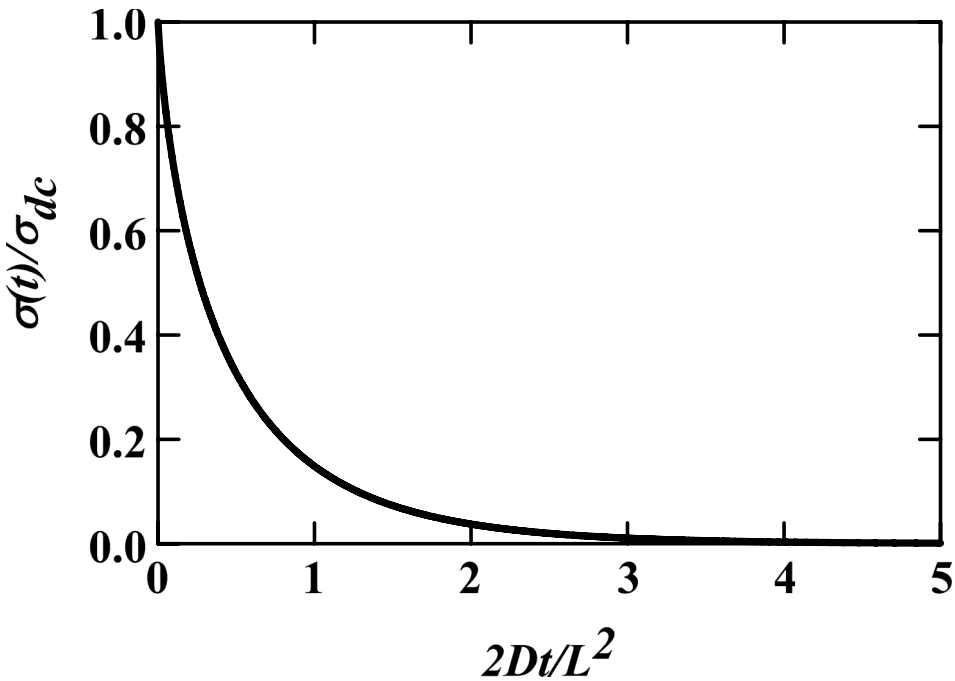

FIG. 2. The conductivity at time t after initiating measurement of the dc conductivity is plotted in units of the intrinsic dc conductivity $\sigma(0) = \sigma_{dc}$ versus t in units of $L^2/2D$, where D and L respectively denote the charge-carriers' diffusion constant and the separation between blocking electrodes.

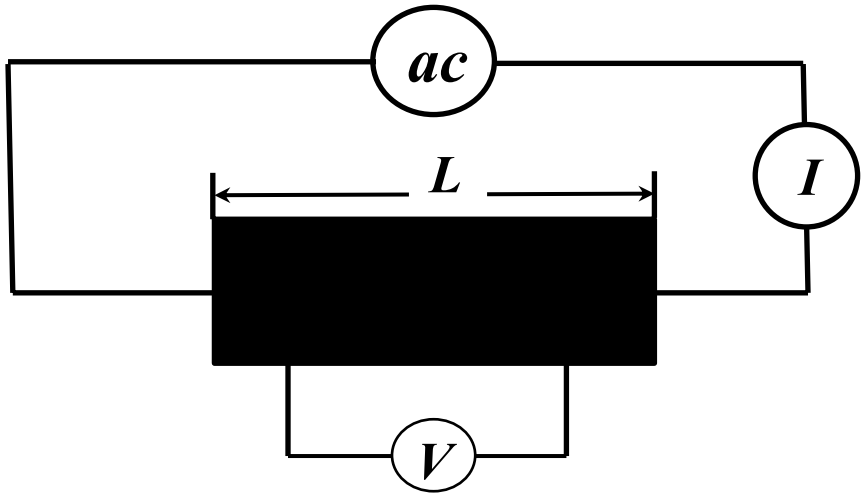

FIG. 3. Schematic illustration of our circuit for measuring the ac conductivity of a sample between blocking electrodes separated by the distance L.

and the strength of the applied electric field, $J(t)$ and E, respectively:

$$Re\left[\sigma\left(\omega\right)\right] \equiv Re\left[\frac{J\left(\omega\right)}{E\left(\omega\right)}\right] = \frac{\int_0^\infty dt\, e^{i\omega t} J\left(t\right)}{E\int_0^\infty dt\, e^{i\omega t}} = \frac{\int_0^\infty dt\, e^{i\omega t} J\left(t\right)}{iE/\omega} = \omega\int_0^\infty dt\sigma\left(t\right) sin\left(\omega t\right). \quad (7)$$

Evaluating this formula for our model yields:

$$Re\left[\sigma\left(\omega\right)\right] = \frac{\sigma_{dc}}{L}\omega\int_0^L dl\int_0^\infty dt\, e^{-2Dt/l^2} sin\left(\omega t\right) = \frac{\sigma_{dc}}{L}\int_0^L dl\left[\frac{\left(\frac{\omega l^2}{2D}\right)^2}{1+\left(\frac{\omega l^2}{2D}\right)^2}\right]$$

$$= \sigma_{dc}\sqrt{\frac{2D}{\omega L^2}}\int_0^{\sqrt{\frac{\omega L^2}{2D}}} dy\left[\frac{y^4}{1+y^4}\right]. \quad (8)$$

Figure 4 displays a plot of Re[σ(ω)] versus $(\omega L^2/2D)^{1/2}$. As expected, Re[σ(ω)] vanishes in the dc limit, $\omega \to 0$, since carriers cannot penetrate the electrodes. However, Re[σ(ω)] remains finite at finite applied frequencies. In particular, Re[σ(ω)] manifests its strongest frequency dependence when $\omega \sim 2D/L^2$. At higher frequencies, $\omega \gg 2D/L^2$, the frequency dependence of the measured conductivity weakens. In this domain the measured conductivity asymptotically approaches the material's intrinsic dc conductivity σ_{dc}:

$$Re\left[\sigma\left(\omega\right)\right] \cong \sigma_{dc}\left[1-\left(\frac{56}{45}\right)\sqrt{\frac{2D}{\omega L^2}}\right]. \quad (9)$$

We have extensively studied samples (~ 1 cm^3) of tissue freshly excised from various brain locations during surgeries on pediatric epilepsy patients.[5,6] Here we summarize some of the salient features of just the bulk conductivity measurements of Refs. 5 and 6. Application of a dc electric field generates a transient conductivity that decays significantly within minutes, $\tau \sim 10^2$ sec. In addition, the ac conductivity measured between 6 – 1000 Hz only increased very slowly with increasing frequency. These results imply that $\tau \sim L^2/2D \gg 1/\omega$. Thus the frequencies of the ac conductivity measurements are too high to observe the relatively slow transient decay. Rather, these ac conductivity measurements simply provide an estimate of the initial dc conductivity: $\sigma_{dc} > \sigma(1000\ \text{Hz})$. The measured dc conductivity at room temperature is $\sigma_{dc} \sim 0.15$ S/m.

The average Na^+ concentration measured in human brain tissue is about 2.4×10^{25} m^{-3} (about 40 mM).[7] A very similar average Na^+ concentration is found in the brain tissue of healthy rats. In

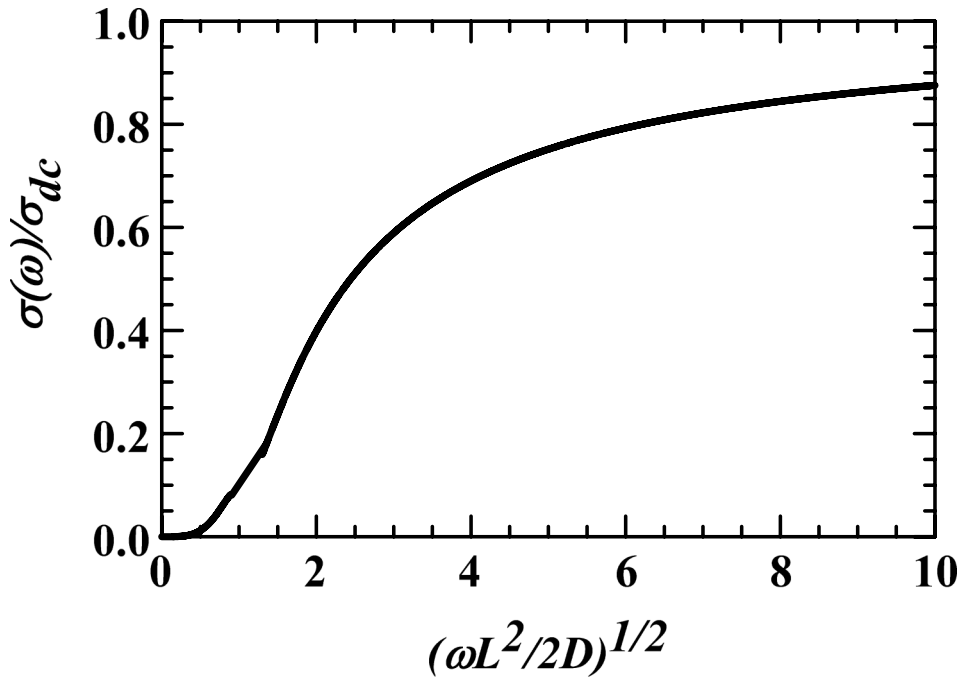

FIG. 4. The ac conductivity, $\sigma(\omega)$ at applied frequency ω, in units of the initial dc conductivity σ_{dc} is plotted versus the square-root of ω in units of $2D/L^2$, where D and L respectively denote the charge-carriers' diffusion constant and the separation between blocking electrodes.

particular, the extracellular and intracellular concentrations of sodium reported for healthy rat brain tissue are 140 mM and 10 mM, respectively, with the extracellular volume fraction being ~ 0.2.[8]

Taken together, the density of Na cations $n_{\rm Na}$ and $\sigma_{\rm dc}$ provide an estimate of their diffusion constant $D_\sigma \equiv [(kT/q)/n_{\rm Na}q]\sigma_{\rm dc}$. In particular, associating our measured dc conductivity with the typical density of human brains' Na cations yields their diffusion constant at room temperature, $kT = 2.5 \times 10^{-2}$ V, $D_\sigma = [(2.5 \times 10^{-2}\ {\rm V})/(2.4 \times 10^{25}\ {\rm m}^{-3})(1.6 \times 10^{-19}\ {\rm C})](1.5 \times 10^{-1}\ {\rm S/m}) \cong 10^{-9}\ {\rm m}^2/{\rm sec}$. In addition, the room-temperature diffusion constants measured with proton-diffusion MRI for the protons of human brain tissue's water molecules are also $\sim 10^{-9}\ {\rm m}^2/{\rm sec}$.[6] This result is not surprising in that the diffusion of Na cations in water is associated with substantial reorientation of some of the surrounding water molecules.[9] Furthermore, diffusion-MRI measurements on Na nuclei in living rat brain also yield anisotropic local apparent diffusion constants of ~ 1 $(\mu{\rm m})^2/{\rm ms} = 10^{-9}\ {\rm m}^2/{\rm sec}$.[8] Similarly, the local anisotropic diffusion constants inferred from proton diffusion-MRI measurements in rat brain are also ~ $10^{-9}\ {\rm m}^2/{\rm sec}$.[10] Thus, the diffusion constant of sodium in freshly excised bulk human brain tissue estimated from measurements of its electrical conductivity is comparable to local values determined non-invasively with MRI and diffusion-MRI.

Attributing the slow transient decay of human brain tissues' dc conductivity to sodium cations moving between blockages provides an estimate of the characteristic separation between them, $L_\sigma \equiv (2D_\sigma\tau)^{1/2}$. With $D_\sigma = 10^{-9}\ {\rm m}^2/{\rm sec}$ and $\tau = 10^2$ sec we find $L_\sigma = (20 \times 10^{-8}\ {\rm m}^2)^{1/2} \cong 4.5 \times 10^{-4}\ {\rm m} = 450\ \mu{\rm m}$. The smallness of L_σ relative to the sample size $L \sim 10^{-2}$ m implies that Na cations' transport is primarily limited by blockages within the material rather than by the experiment's electrodes. For example, ions diffusing through intercellular fluid must navigate through a dense distribution of cells with diameters up to 40 μm.[10,11] All told, sodium cations would appear to tortuously diffuse among many cells in the brain's complex inhomogeneous medium before being effectively blocked.

In summary, we addressed the temporal decay of ionic charge carriers' dc conductivity and the associated ac conductivity that results from simple blockages. The analysis has been applied to electrical conductivity measurements 1) on bulk NaCl-doped gelatin gels that are commonly employed proxies for brain tissue and 2) on actual freshly excised bulk brain tissue. The temporal

decay of the conductivities of our NaCl-doped gelatin gels appear extrinsic, $L_\sigma > L$, dominated by ions encountering impenetrable electrodes separated by 1 cm. By contrast, the temporal decay of our conductivity measurements of freshly excised bulk brain tissue appears intrinsic, $L_\sigma < L$, dominated by effective blockages separated by about 450 microns. These microstructural blockages impede ionic transport through complex inhomogeneous bulk brain tissue.

ACKNOWLEDGEMENTS

These studies were supported by NIH R21 NS060675-01 and NIH RO1 NS38992 and the Weil Fund at UCLA Semel Institute for Neuroscience and Human Behavior

[1] M. Pollak and T. H. Geballe, Phys. Rev. **122**, 1742 (1961).
[2] D. Emin, Phys. Rev. B **46**, 9419 (1992).
[3] L. E. Reichl, *A Modern Course in Statistical Mechanics* (University of Texas Press, Austin, 1980), Chap. 6.D.
[4] M. Abramowitz and I. A. Stegun, *Handbook of Mathematical Functions*, National Bureau of Standards Applied Mathematics Series Vol. 55 (1964).
[5] M. Akhtari, N. Salamon, R. Duncan, I. Fried, and G. W. Mathern, Brain Topogr. **18**, 281 (2006).
[6] M. Akhtari, M. Mandelkern, D. Bui, N. Salamon, H. V. Vinters, and G. W. Mathern, Brain Topogr. **23**, 292 (2010).
[7] G. Madelin, R. Kline, R. Walvick, and R. R. Regatte, Scientific Reports **4**, 4763 (2014).
[8] J. A. Goodman, C. D. Kroenke, G. L. Bretthorst, J J. H. Ackerman, and J. J. Neil, Magnetic Resonance in Medicine **53**, 1040 (2005).
[9] B. Hirbar, N. T. Southhall, V. Vlachy, and K. A. Dill, J. Am. Chem. Soc. **124**, 12302 (2002).
[10] M. Sekino, H. Ohsaki, S. Yamaguchi-Sekino, N. Iriguchi, and S. Ueno, Bioelectromagnetics **30**, 489 (2009).
[11] J. Holsheimer, Exp. Brain Res. **6**(7), 402 (1987).